


Spatial Clustering of Depinning Avalanches in Presence of Long-Range Interactions

Clément Le Priol¹, Pierre Le Doussal¹ and Alberto Rosso²

¹Laboratoire de Physique de l'École Normale Supérieure, Université PSL, CNRS, Sorbonne Université, Université de Paris, 24 rue Lhomond, 75231 Paris Cedex, France

²LPTMS, CNRS, Université Paris-Sud, Université Paris-Saclay, 91405 Orsay, France

 (Received 25 August 2020; revised 14 October 2020; accepted 11 December 2020; published 12 January 2021)

Disordered elastic interfaces display avalanche dynamics at the depinning transition. For short-range interactions, avalanches correspond to compact reorganizations of the interface well described by the depinning theory. For long-range elasticity, an avalanche is a collection of spatially disconnected clusters. In this Letter we determine the scaling properties of the clusters and relate them to the roughness exponent of the interface. The key observation of our analysis is the identification of a Bienaymé-Galton-Watson process describing the statistics of the number of clusters. Our work has concrete importance for experimental applications where the cluster statistics is a key probe of avalanche dynamics.

DOI: [10.1103/PhysRevLett.126.025702](https://doi.org/10.1103/PhysRevLett.126.025702)

Many catastrophic phenomena such as epidemic outbreaks, earthquakes [1–3], or financial crashes are initiated by a single unstable seed that destabilizes many other elements. The instability propagates as a cascade where each unstable element triggers a number of offsprings. These processes are also observed in the response of disordered systems to small perturbations and are called avalanches [4]. The cascades of plastic events in amorphous materials [5,6], the ground-state reorganizations of mean-field spin glasses [7,8] or the jerky motion of fronts propagating in heterogeneous media [9,10] are examples of such avalanches.

We can consider that the first model of avalanches was introduced by Bienaymé [11] and by Galton and Watson [12] who were interested in the extinction probability of surnames. In this model the number of offspring per individual is an independent identically distributed random variable whose average R_0 determines the fate of the process. If $R_0 > 1$ there is a finite probability that the surname never gets extinct, while for $R_0 \leq 1$ the surname gets extinct with probability one. In this case the family size S (total number of descendants of an individual) is a stochastic variable displaying a power law distribution $P(S) \sim S^{-\tau}$, with exponent $\tau = 3/2$, which is truncated (exponentially) above a maximal size $S_m \sim (1 - R_0)^{-2}$.

We are interested in the avalanches observed when elastic interfaces of dimension d , such as magnetic domain walls [13–15], crack fronts [16–20], imbibition fronts [21,22], or wetting lines [23–27] propagate in heterogeneous materials. Under the action of an external force f , the front remains pinned up to a critical force f_c where it undergoes a depinning transition. At the depinning point the front is in a self-affine configuration characterized by the roughness exponent ζ , whose value is known from numerical simulations [28,29] and functional renormalization group (FRG)

calculations [30–33]. Near depinning, small perturbations can trigger avalanches which are large rearrangements of the front, of total size S . In the presence of short-range (SR) elasticity, avalanches are spatially connected and the size exponent τ is smaller than the one predicted by the Bienaymé-Galton-Watson (BGW) model. Indeed spatial information is absent from the BGW model while one expects that, for an unstable point of the interface, the analog of the number of offspring depends on its generation and its position. Moreover, the avalanche of an interface has a spatial location characterized by a linear size ℓ that displays a power law distribution $P(\ell) \sim \ell^{-\kappa}$.

In many physical situations, fronts are, however, characterized by a long-range (LR) elastic kernel that decays as $1/r^{d+\alpha}$. In particular it has been shown that the elasticity of crack fronts [16,34] and wetting lines [23] is LR with $\alpha = 1$. The shape of the interface is affected by the range of the interactions. As a function of α we identify three regimes: (i) the mean-field (MF) case, for $\alpha \leq d/2$, where the interface is flat and $\zeta = 0$, (ii) for $d/2 < \alpha < 2$ the interface is rough and ζ grows with α , (iii) for $\alpha \geq 2$, ζ saturates to its SR value, ζ_{SR} . For LR interactions with $d/2 \leq \alpha \leq 2$ the depinning predicts that $S \sim \ell^{d+\zeta}$ and that the avalanche exponents are not independent but related to the roughness exponent via the relations [13,31,35]

$$\tau = 2 - \frac{\alpha}{d + \zeta}, \quad \kappa = 1 + d + \zeta - \alpha \quad \text{for } \frac{d}{2} \leq \alpha \leq 2. \quad (1)$$

For $\alpha > 2$ the equations saturate to $\tau = 2 - 2/(d + \zeta_{\text{SR}})$, $\kappa = d + \zeta_{\text{SR}} - 1$, while in the MF case we recover the BGW exponent $\tau = 3/2$. LR avalanches are qualitatively different from SR ones as they are in general disconnected objects. An example of an avalanche for $\alpha = 1$ is shown in Fig. 1. It is composed of N_c disconnected clusters.

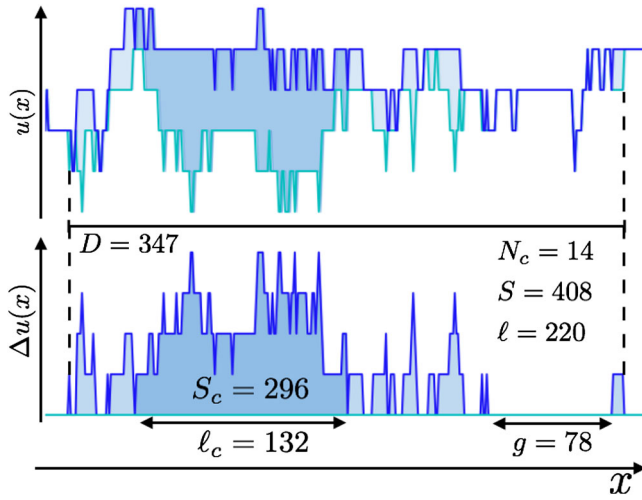


FIG. 1. Top: LR ($\alpha = 1$) avalanche of a front $u(x)$ moving between two stable configurations. The area swept by the line is the avalanche size S . Bottom: Relative displacement $\Delta u(x)$ of the final configuration with respect to the initial one. The avalanche is made of N_c distinct clusters.

We denote S_c the size of a given cluster, and ℓ_c its extension. A gap between two clusters is denoted by g . We define the linear size of the avalanche as $\ell = \sum \ell_c$. This length is much shorter than the diameter D of the avalanche (i.e., the maximal distance between two points which have moved during the avalanche).

These quantities display power law statistics that are important to characterize. Indeed, in experiments where the spatial structure is accessible, independently triggered avalanches can overlap in time and/or space [36–40] so that only clusters remain simple to identify.

The first attempt to characterize the cluster statistics of LR depinning avalanches was done in Ref. [41], where, based on numerical simulations for $\alpha = 1$, a scaling relation for the cluster size exponent was proposed and justified by arguments that we show to be incorrect. This relation was experimentally confirmed in Ref. [37] for $\alpha = 1$. In this Letter we derive scaling relations for all cluster exponents, and for all $d/2 \leq \alpha \leq 2$ and show that they depend only on

the roughness exponent ζ (our results are gathered in Table I). The validity of our relations is based on the key numerical observation, unveiled here, that the distribution of N_c appears to obey the same statistics as the total number of descendants in the BGW model.

Let us start by defining the cellular automaton model, already used in Refs. [40–42], for the simulations of depinning interfaces. Consider a line ($d = 1$) $u(x, t)$ where t is the time, x the internal coordinate and u the displacement field (see Fig. 1). We assume that all variables t, x , and u are integers, that the line size is L and we implement periodic boundary conditions $u(x + L, t) = u(x, t)$. The disorder pins the line up to a local threshold force $\eta^{\text{th}}[x, u]$ balanced by the force

$$F(x, t) = m^2[w - u(x, t)] + \sum_{x'} \frac{u(x', t) - u(x, t)}{|x' - x|^{1+\alpha}}, \quad (2)$$

where the first term describes the driving force $f(x, t) = m^2[w - u(x, t)]$ deriving from a harmonic confinement of curvature m^2 and the second is the LR elastic force. The local thresholds $\eta^{\text{th}}[x, u]$ are independent identically distributed random numbers drawn from the positive part of a normal distribution. The harmonic confinement induces maximal sizes $\ell_m \sim m^{-2/\alpha}$ and $S_m \sim \ell_m^{d+\zeta}$ above which the power law distributions $P(\ell) \sim \ell^{-\kappa}$ and $P(S) \sim S^{-\tau}$ are truncated. It sets the distance from the critical point (at $m = 0$) and corresponds to $m^2 \sim 1 - R_0$ in the BGW model. At time t if $F(x, t) < \eta^{\text{th}}[x, u(x, t)]$ the point is stable while if $F(x, t) \geq \eta^{\text{th}}[x, u(x, t)]$ the point is unstable: it topples, namely, $u(x, t + 1) = u(x, t) + 1$, and the new threshold $\eta^{\text{th}}[x, u + 1]$ is drawn. Avalanches are produced in a quasistatic protocol: when all points are stable w is increased up to a value at which a first instability occurs and the dynamics unfolds until the line reaches a new stable configuration. We focus on the stationary regime of avalanches, reached after a transient when starting from an arbitrary configuration. Our simulations are performed for a line of size $L = 2^{17}$ for $\alpha = 0.5, 0.75, 1$, and 1.5 and many

TABLE I. Table of exponents. The measured values correspond to best fits of our data. The predictions correspond to the scaling relations indicated in the third column [obtained by combining Eqs. (1), (3), (5), and (8)], for $d = 1$, using the values of ζ listed in the first line.

Exponent	Expression	Relation	measured/prediction			
			$\alpha = 0.5$	$\alpha = 0.75$	$\alpha = 1$	$\alpha = 1.5$
ζ	$S(q) \sim q^{-(d+2\zeta)}$		0 (MF)	0.18(1)	0.39 [28]	0.75(2)
γ_S	$\langle N_c \rangle_S \sim S^{\gamma_S}$	$\gamma_S = 2 - 2\alpha/(d + \zeta)$	0.89(2)/1	0.73(1)/0.73(1)	0.52(2)/0.56	0.29(1)/0.28(2)
γ_ℓ	$\langle N_c \rangle_\ell \sim S^{\gamma_\ell}$	$\gamma_\ell = 2(d + \zeta - \alpha)$	0.93(2)/1	0.80(2)/0.86(2)	0.70(2)/0.78	0.50(2)/0.54(4)
τ	$P(S) \sim S^{-\tau}$	$\tau = 2 - \alpha/(d + \zeta)$	1.50(1)/ $\frac{3}{2}$	1.36(2)/1.36(1)	1.26(2)/1.28	1.14(2)/1.14(1)
τ_c	$P(S_c) \sim S_c^{-\tau_c}$	$\tau_c = 3 - 2\alpha/(d + \zeta)$	2.00(9)/2	1.72(4)/1.73(1)	1.56(2)/1.56	1.28(2)/1.28(2)
κ	$P(\ell) \sim S^{-\kappa}$	$\kappa = 1 + d + \zeta - \alpha$	1.50(2)/ $\frac{3}{2}$	1.38(5)/1.43(1)	1.33(5)/1.39	1.20(3)/1.25(2)
κ_c	$P(\ell_c) \sim S_c^{-\kappa_c}$	$\kappa_c = 1 + 2(d + \zeta - \alpha)$	2.05(5)/2	1.90(5)/1.86(2)	1.80(2)/1.78	1.45(3)/1.50(4)

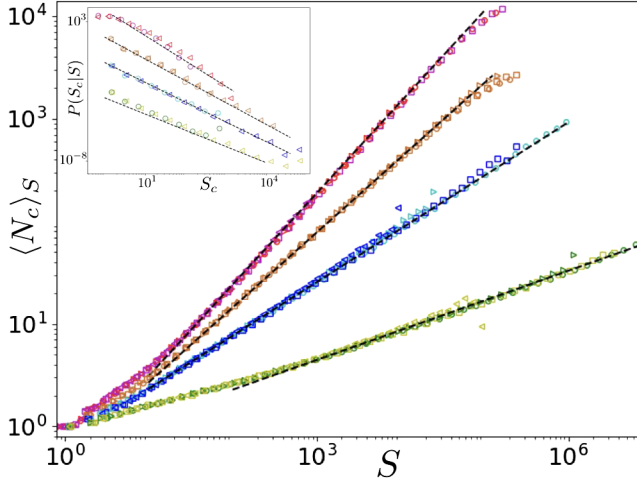


FIG. 2. Main panel: $\langle N_c \rangle_S$ versus S for $\alpha = 0.5, 0.75, 1$, and 1.5 (top to bottom). Dashed lines fit the exponent γ_S , values listed in Table I. Inset: $P(S_c|S)$ for $S = 10^3$ (circles) and $S = 10^5$ (triangles). Dashed lines correspond to the exponents τ_c of $P(S_c)$ measured in the Supplemental Material [43]. (Data are shifted vertically.)

values of the curvature for each α . The details of the parameters are given in the Supplemental Material [43].

This model was implemented in Ref. [41] for $\alpha = 1$ and the analysis of the data led to conjecture the following scaling relation for the cluster size exponent τ_c :

$$\tau_c = 2\tau - 1. \quad (3)$$

The justification of this relation was based on two assumptions: (i) During the avalanche spreading the evolution of the number of clusters is interpreted as a discrete random walk with the time replaced by the number of topplings. At each time step, the number of clusters can increase by 1, remain constant, or decrease by 1. This implies that the average number of clusters at the end of avalanches of size S (equal to the total number of topplings) scales as $\langle N_c \rangle_S \sim S^{\gamma_S}$. The assumption that the process is Markovian leads to $\gamma_S = 1/2$. (ii) The clusters belonging to an avalanche of size S have a typical size $S_c \sim S/\langle N_c \rangle_S \sim S^{1-\gamma_S}$ and applying $P(S_c)dS_c = P(S)dS$ one finds [44]

$$\tau_c = \frac{\tau - \gamma_S}{1 - \gamma_S}, \quad (4)$$

which yields Eq. (3) for $\gamma_S = 1/2$. In the case $\alpha = 1$, the value of γ_S was found numerically to be compatible with $1/2$. In Fig. 2 we extend the study to $1/2 \leq \alpha < 2$. We find that in general $\gamma_S \neq 1/2$ and that it decreases continuously with α . Inserting our measured values of γ_S in Eq. (4) yields predictions for τ_c that differ from the observed values [e.g., for $\alpha = 0.75$ we measured $\gamma_S = 0.73$ and $\tau_c = 1.72$ while Eq. (4) yields $\tau_c = 2.33$]. Equation (4) is wrong as the assumption (ii) is incorrect: clusters belonging to

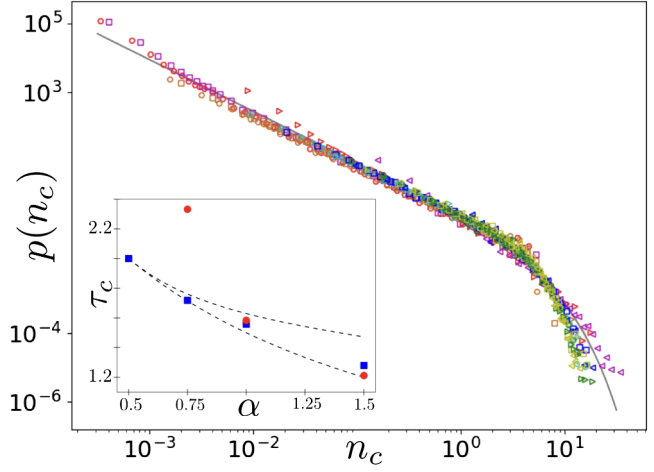


FIG. 3. Main panel: $p(n_c)$ for $\alpha = 0.5, 0.75, 1$, and 1.5 . The thin gray line corresponds to p_{BGW} (7). Inset: Direct measurements of τ_c (blue squares) compared with (i) the prediction (4) using the fitted values of γ_S (red circles); (ii) our prediction of τ_c as a function of ζ (see Table I) using FRG predictions $\zeta^{1\text{loop}}$ [32,33] (bottom line) and $\zeta^{2\text{loop}}$ [33] (upper line) given in the Supplemental Material [43].

avalanches of size S do not have the same typical size but are broadly distributed according to a power law distribution $P(S_c|S) \sim S_c^{-\tau_c}$ for S_c up to S (see inset in Fig. 2). This implies that $\langle S_c \rangle_S \sim S^{2-\tau_c}$. Using $\langle N_c \rangle_S = S/\langle S_c \rangle_S$ we obtain $\langle N_c \rangle_S \sim S^{\tau_c-1}$ and thus

$$\tau_c = \gamma_S + 1. \quad (5)$$

In Fig. 3 we study the statistics of the number of clusters for different values of α and m^2 . A collapse for different values of m^2 is obtained by introducing the variable $n_c = 2N_c \times \langle N_c \rangle / \langle N_c^2 \rangle$ and computing $p(n_c)$ defined as [45,46]

$$p(n_c)dn_c = \frac{\langle N_c^2 \rangle}{2\langle N_c \rangle^2} P(N_c)dN_c. \quad (6)$$

The expression of $p(n_c)$ is known for BGW [47,48]:

$$p_{\text{BGW}}(n_c) = \frac{n_c^{-3/2}}{2\sqrt{\pi}} \exp(-n_c/4). \quad (7)$$

The main panel of Fig. 3 presents a remarkable collapse of the data on the same universal curve for all α and cannot be clearly distinguished from the BGW function of Eq. (7). In the case $\alpha = 0.5$ one expects that the number of clusters is proportional to the avalanche size (up to logarithmic corrections). Thus it is not too surprising to recover a BGW shape in this case, since, in mean field, this is the distribution of the avalanche size. It is, however, much less clear why this behavior should hold for $\alpha > 0.5$. Numerically we cannot exclude that $p(n_c)$ is BGW

(in the limit $m \rightarrow 0$, $L \rightarrow \infty$) also for $\alpha = 0.75$, $\alpha = 1$ and $\alpha = 1.5$. However, for what follows we need only to assume that $P(N_c) \sim N_c^{-3/2}$ and we do not mind about the exact decay at large scale. To conclude the argument it is sufficient to remark that $P(N_c)dN_c = P(S)dS$ (see Supplemental Material [43] for an equivalent derivation) which yields $\gamma_S = 2(\tau - 1)$. Combined with the relation (5), we arrive at the scaling relation (3) which we thus find to be valid for all α , by a completely different mechanism from Ref. [41]. Note that we can also infer that the cutoff of $P(N_c)$ scales as $N_m \sim S_m^{\tau_c - 1}$.

The same reasoning can be repeated to find the relation between the extension ℓ of an avalanche and the extension ℓ_c of the clusters. Using the definition for γ_ℓ , $\langle N_c \rangle \ell \sim \ell^\gamma$, we first derive the relation $\gamma_\ell = \kappa_c - 1$. Then using $P(N_c) \sim N_c^{-3/2}$ and $P(N_c)dN_c = P(\ell)d\ell$ we derive

$$\kappa_c = 2\kappa - 1. \quad (8)$$

Note that from $\gamma_S = \tau_c - 1$, $\gamma_\ell = \kappa_c - 1$ and $N_c^{1/\gamma_S} \sim S \sim \ell^{d+\zeta} \sim N_c^{(d+\zeta)/\gamma_\ell}$ we deduce $\kappa_c - 1 = (\tau_c - 1)(d + \zeta)$. This corresponds to the self-affinity of the clusters $S_c \sim \ell_c^{d+\zeta}$ which is checked in the Supplemental Material [43].

The scaling relations that we have derived allow us to express all the exponents as functions of ζ and α . We have collected all these expressions in Table I and compared the predicted values of the exponents with the ones directly measured in our numerical simulations. We found good agreements for all values of α .

Note that at variance with SR elasticity the diameter D does not coincide with the avalanche linear size ℓ but is in general much larger. Therefore it displays novel statistical properties that we should characterize. In Fig. 4 we show the diameter distribution for $\alpha = 0.5, 1$, and 1.5 . For $\alpha > 0.5$ a crossover $D_{\text{cross}} \sim \ell_m$ separates two power law decays:

$$P(D) \sim \begin{cases} D^{-\kappa_D} & \text{for } D \ll D_{\text{cross}}, \\ D^{-(d+\alpha)} & \text{for } D \gg D_{\text{cross}}. \end{cases} \quad (9)$$

Remarkably, the exponent κ_D is α independent with a numerical value close to 1.2 (also for $\alpha = 0.5$) in $d = 1$. The decay for $D \gg D_{\text{cross}}$ originates from the LR elasticity and should hold for any d . The statistics of the diameter is very different from the one of the linear size ℓ . Since $D = \ell + G$, where $G = \sum g$ is the total gap, we need to investigate the statistics of the gaps g in order to understand the statistics of the diameter. Their distributions, shown in the inset of Fig. 4, present a crossover $g_{\text{cross}} \simeq 10\ell_m$ between two power law decays:

$$P(g) \sim \begin{cases} g^{-\kappa_g} & \text{for } g \ll g_{\text{cross}}, \\ g^{-(d+\alpha)} & \text{for } g \gg g_{\text{cross}}, \end{cases} \quad (10)$$

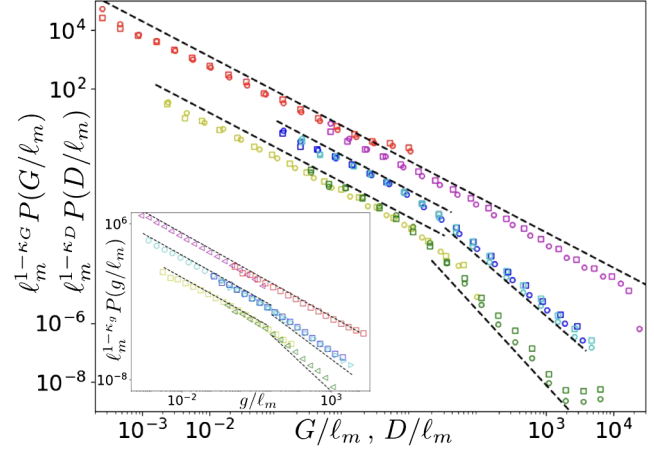


FIG. 4. Main panel: Diameter (circles) and total gap length (squares) distributions for $\alpha = 0.5, 1$, and 1.5 . We used $\ell_m = m^{-2/\alpha}$. Dashed lines are fits with exponents $\kappa_D = 1.2$ at small scales and $d + \alpha$ at large scales for $\alpha = 1$ and 1.5 . Inset: Gap distributions. The dashed lines are guides to the eye for exponents $\kappa_g = 3/2$ at small scale and $d + \alpha$ at large scale.

with $\kappa_g = 3/2$ independently from α . Since the decay of $P(g)$ is much slower than the one of $P(\ell_c)$ (which decays faster than any power law at large scale, see Supplemental Material [43]), we expect $G \gg \ell$ which implies that $D \simeq G$. This latter relation is confirmed by Fig. 4 where the distribution of D and G are plotted together and are indistinguishable.

The scaling form (9) can now be derived from the gap distribution (10). Let us first consider avalanches where all gaps are below g_{cross} . In this case we can write

$$\langle N_c \rangle_G = 1 + \frac{G}{\langle g \rangle_G} \sim G^{\kappa_g - 1} \simeq D^{\kappa_g - 1}, \quad (11)$$

where we used $\langle g \rangle_G \sim G^{2-\kappa_g}$ since $P(g|G) \sim g^{-\kappa_g}$ for g up to G (see Supplemental Material [43]). Again using $P(N_c) \sim N_c^{-3/2}$ and setting $P(N_c)dN_c = P(D)dD$ we find

$$\kappa_D = (\kappa_g + 1)/2 \simeq 1.25, \quad (12)$$

which is close from the exponent we measure $\kappa_D \simeq 1.2$. For very large D , we assume the existence of a gap $g \sim D \gg g_{\text{cross}}$. This gap has a probability $\propto g^{-(d+\alpha)}$ leading to the tail $\propto D^{-(d+\alpha)}$.

The main result of this Letter is to show that, even in presence of LR interactions, the statistical properties of depinning avalanches can always be expressed as functions of α and ζ . Our conclusions are based on the numerical observation that the number of clusters behave as the number of offspring of a BGW model for all α between $1/2$ and 2 . We are not able to demonstrate this conjecture but our numerics shows that it is a very good approximation. All relations between the exponents of clusters and global

avalanches are based on this conjecture so it would be of great interest to show it analytically. $P(N_c)$ can also be studied experimentally thanks to a new method introduced in Ref. [22]. These relations have been tested in $d = 1$ but we believe that they also hold for $d > 1$. It would be also interesting to characterize the statistical properties of the clusters of plastic avalanches [5,6,49,50]. Indeed the Eshelby kernel, which is the relevant interaction for the yielding transition, is long-range (with $\alpha = 0$) but, in contrast with depinning, nonmonotonous.

We thank L. Ponsou for enlightening discussions. P.L.D. acknowledges support from ANR under Grant No. ANR-17-CE30-0027-01 RaMaTraF.

-
- [1] D. S. Fisher, K. Dahmen, S. Ramanathan, and Y. Ben-Zion, *Phys. Rev. Lett.* **78**, 4885 (1997).
- [2] E. A. Jagla, F. P. Landes, and A. Rosso, *Phys. Rev. Lett.* **112**, 174301 (2014).
- [3] L. de Arcangelis, C. Godano, J. R. Grasso, and E. Lippiello, *Phys. Rep.* **628**, 1 (2016).
- [4] J. P. Sethna, K. A. Dahmen, and C. R. Myers, *Nature (London)* **410**, 242 (2001).
- [5] J. Lin, E. Lerner, A. Rosso, and M. Wyart, *Proc. Natl. Acad. Sci. U.S.A.* **111**, 14382 (2014).
- [6] J.-C. Baret, D. Vandembroucq, and S. Roux, *Phys. Rev. Lett.* **89**, 195506 (2002).
- [7] P. Le Doussal, M. Müller, and K. J. Wiese, *Phys. Rev. B* **85**, 214402 (2012).
- [8] S. Franz and S. Spigler, *Phys. Rev. E* **95**, 022139 (2017).
- [9] D. S. Fisher, *Phys. Rep.* **301**, 113 (1998).
- [10] M. Kardar, *Phys. Rep.* **301**, 85 (1998).
- [11] I.-J. Bienaimé, *Soc. Philomat. Paris Extraits Sér.* **5**, 4 (1845).
- [12] H. W. Watson and F. Galton, *J. Anthropol. Inst. Great Br. Ireland* **4**, 138 (1875).
- [13] S. Zapperi, P. Cizeau, G. Durin, and H. E. Stanley, *Phys. Rev. B* **58**, 6353 (1998).
- [14] L. Laurson, X. Illa, S. Santucci, K. T. Tallakstad, K. J. Måløy, and M. J. Alava, *Nat. Commun.* **4**, 2927 (2013).
- [15] G. Durin, F. Bohn, M. A. Corrêa, R. L. Sommer, P. Le Doussal, and K. J. Wiese, *Phys. Rev. Lett.* **117**, 087201 (2016).
- [16] H. Gao and J. Rice, *J. Appl. Mech. Trans. ASME* **56**, 828 (1989).
- [17] A. Tanguy, M. Gounelle, and S. Roux, *Phys. Rev. E* **58**, 1577 (1998).
- [18] D. Bonamy, S. Santucci, and L. Ponsou, *Phys. Rev. Lett.* **101**, 045501 (2008).
- [19] D. Bonamy and E. Bouchaud, *Phys. Rep.* **498**, 1 (2011).
- [20] L. Ponsou, *Int. J. Fract.* **201**, 11 (2016).
- [21] M. Pradas, J. M. López, and A. Hernández-Machado, *Phys. Rev. E* **80**, 050101(R) (2009).
- [22] R. Planet, J. M. López, S. Santucci, and J. Ortín, *Phys. Rev. Lett.* **121**, 034101 (2018).
- [23] J. F. Joanny and P. G. de Gennes, *J. Chem. Phys.* **81**, 552 (1984).
- [24] S. Roux, D. Vandembroucq, and F. Hild, *Eur. J. Mech.* **22**, 743 (2003).
- [25] S. Moulinet, A. Rosso, W. Krauth, and E. Rolley, *Phys. Rev. E* **69**, 035103(R) (2004).
- [26] P. Le Doussal, K. Wiese, S. Moulinet, and E. Rolley, *Europhys. Lett.* **87**, 56001 (2009).
- [27] P. Le Doussal and K. J. Wiese, *Phys. Rev. E* **82**, 011108 (2010).
- [28] A. Rosso and W. Krauth, *Phys. Rev. E* **65**, 025101(R) (2002).
- [29] A. Rosso, A. K. Hartmann, and W. Krauth, *Phys. Rev. E* **67**, 021602 (2003).
- [30] T. Nattermann, S. Stepanow, L.-H. Tang, and H. Leschhorn, *J. Phys. II (France)* **2**, 1483 (1992).
- [31] O. Narayan and D. S. Fisher, *Phys. Rev. B* **48**, 7030 (1993).
- [32] D. Ertaş and M. Kardar, *Phys. Rev. E* **49**, R2532 (1994).
- [33] P. Le Doussal, K. J. Wiese, and P. Chauve, *Phys. Rev. B* **66**, 174201 (2002).
- [34] J. R. Rice, *J. Appl. Mech.* **52**, 571 (1985).
- [35] A. Dobrinevski, P. L. Doussal, and K. J. Wiese, *Europhys. Lett.* **108**, 66002 (2014).
- [36] K. J. Måløy, S. Santucci, J. Schmittbuhl, and R. Toussaint, *Phys. Rev. Lett.* **96**, 045501 (2006).
- [37] K. T. Tallakstad, R. Toussaint, S. Santucci, J. Schmittbuhl, and K. J. Måløy, *Phys. Rev. E* **83**, 046108 (2011).
- [38] J. Barés, L. Barbier, and D. Bonamy, *Phys. Rev. Lett.* **111**, 054301 (2013).
- [39] S. Janičević, L. Laurson, K. J. Måløy, S. Santucci, and M. J. Alava, *Phys. Rev. Lett.* **117**, 230601 (2016).
- [40] C. Le Priol, J. Chopin, P. Le Doussal, L. Ponsou, and A. Rosso, *Phys. Rev. Lett.* **124**, 065501 (2020).
- [41] L. Laurson, S. Santucci, and S. Zapperi, *Phys. Rev. E* **81**, 046116 (2010).
- [42] J. Schmittbuhl, S. Roux, J.-P. Vilotte, and K. J. Måløy, *Phys. Rev. Lett.* **74**, 1787 (1995).
- [43] See Supplemental Material at <http://link.aps.org/supplemental/10.1103/PhysRevLett.126.025702> for details about the parameters, the measurement of the exponents and the derivations of the scaling relations.
- [44] For convenience, here and below we use the same letter P to denote the probability densities of all observables.
- [45] A. Rosso, P. Le Doussal, and K. J. Wiese, *Phys. Rev. B* **80**, 144204 (2009).
- [46] Note that $p(n_c)$ is not a probability distribution function.
- [47] P. Le Doussal, A. A. Middleton, and K. J. Wiese, *Phys. Rev. E* **79**, 050101(R) (2009).
- [48] P. Le Doussal and K. J. Wiese, *Phys. Rev. E* **79**, 051106 (2009).
- [49] K. M. Salerno, C. E. Maloney, and M. O. Robbins, *Phys. Rev. Lett.* **109**, 105703 (2012).
- [50] A. Nicolas, E. E. Ferrero, K. Martens, and J.-L. Barrat, *Rev. Mod. Phys.* **90**, 045006 (2018).